




# Estimation and prediction of riverbank erosion and accretion rate using DSAS, BEHI, and REBVI models: evidence from the lower Ganga River in India

Md Hasanuzzaman<sup>1</sup> · Biswajit Bera<sup>2</sup> · Aznarul Islam<sup>3</sup> · Pravat Kumar Shit<sup>1</sup> 

Received: 20 November 2021 / Accepted: 31 May 2023 / Published online: 12 June 2023  
© The Author(s), under exclusive licence to Springer Nature B.V. 2023

## Abstract

The process of riverbank erosion is often accelerated by natural events and anthropogenic activities leading to the transformation of this natural process to natural hazard. The present study aims to calculate past, present, and future riverbank erosion and accretion (EA) rates using an automated digital shoreline analysis system (DSAS) model of the lower part of the Ganga River in India. Moreover, this study evaluated the EA with bank erosion hazard index (BEHI) and river embankment breaching vulnerability index (REBVI). In this study, satellite images (1973, 1987, 1997, 2007, and 2020) were used for EA rates calculation and field survey data (bank materials, geotechnical parameters, embankment structure, hydraulic pressure, etc.) were used for BEHI and REBVI scores calculation. From 1973 to 2020, the average bank EA rate was found to be 0.119 km/year and 0.046 km/year at the left bank and 0.052 km/year and 0.066 at the right bank. During this period, six villages/mouza (smallest administrative unit of India for revenue collection) were very highly vulnerable due to very high left bank erosion. The long-term prediction (2020–2045) estimates that the average EA rate will be 0.164 km/year and 0.021 km/year at the left bank and 0.031 km/year and 0.045 km/year at the right bank. From this period, 21 villages were highly vulnerable due to very high left bank erosion. Moreover, BEHI and REBVI scores were very high in these villages. RMSE, Student's *t*-test, and  $R^2$  statistical techniques were used for DSAS model validation. Therefore, RMSE (from 0.103 to 0.247), Student's *t*-test, and  $R^2$  (0.82 for the left bank and 0.79 for the right bank) values justified the acceptance of the model. This study may help decision makers as the spatial guidelines to understand future trends of riverbank EA rates for land-use planning and management strategies to protect riverbanks.

**Keywords** Erosion–accretion · DSAS model · BEHI · REBVI · Alluvial channel · Remote sensing

## 1 Introduction

The Ganga River is the second largest river in terms of sediment transport in the world, which covers 1.09 million km<sup>2</sup> basin areas (Dewan et al. 2017). This river has flowed through different types of landforms, and when passing through the deltaic region, the river adjusts itself very dynamically by the erosion and accretion (Bera et al 2019). The Farakka barrage has been constructed in 1975 across the Ganga River in between the Malda and Murshidabad districts of West Bengal in India (Islam and Guchhait 2017). It made important changes in the hydrological, morphological, patterns, and sedimentological characteristics of the lower part of the Ganga River (Bera et al 2019). However, some major problems (massive riverbank erosion, high rate of bar formation, flood, etc.) are raised in this part of the river due to this construction (Guchhait et al 2016). About 4.5 lakh people from 40 villages lost their residence in the Malda district (Talukdar et al. 2021). About 42.74 km<sup>2</sup> area was eroded in this part of the Ganga River by the left bank riverbank erosion during 1979 to 2004 (Das and Samanta 2022), which resulted in the continuous loss of residential areas, agricultural land, roads, infrastructure, and schools building. It made a crucial impact on the physical landscape as well as demographic and socio-economic structure (Hasanuzzaman et al. 2022a). Such problems induce regional backwardness, and local communities are lagging behind the mainstream society that hinders India from achieving the sustainable development. Thus, there is an urgent need to develop an appropriate management plan through scientific research.

Therefore, many researchers have been investigating on this region by using various methods and techniques (Table 1). However, the most of the researchers applied the traditional technique and manual overlapping method to calculate the Ganga River bank erosion and accretion (EA). Traditional technique or manual overlapping methods have a high chance of possibility of human bias and errors (Ashraf and Shakir 2018; Jana 2019). Because they were manually calculated. Over time, as new scientific methods emerge, so to do novel ways of measuring riverbank erosion, and with the advent of modern automated techniques, the likelihood of human bias has significantly decreased compared with the traditional manual overlapping method. Moreover, a very low number of transects was presented (mostly 15–20) with a spacing of 5–10 km. Therefore, the present study applied a statistical-based automated digital shoreline analysis system (DSAS) model for the estimation and prediction of riverbank erosion–accretion rate. In this model, around 1400 auto-generated transects were used with the 50-m spacing. This model automatically calculates the EA rate using banklines. Thus, the possibility of human bias and error is very low. Through an in-depth analysis of the existing literature, it can be confidently stated that with the exception of the DSAS model, all currently available models for calculating riverbank erosion and accretion are manually operated. Therefore, the DSAS model is the only automated tool available for calculating riverbank erosion and accretion. Moreover, in the field of riverbank erosion and accretion, there are no models available that can predict future changes aside from the DSAS model.

DSAS is a highly acceptable and popular method that was developed by the United States Geological Survey (USGS). It is capable of accurately measuring the rate and prediction of different river bankline positions (right and left bank separately) (Thieler et al. 2009; Ashraf and Shakir 2018; Jana 2019; Hasanuzzaman et al. 2022b). Many researchers have successfully applied the DSAS model in their fields such as Hapke et al. (2009) in the USA, Hai-Hoa et al. (2013) in Vietnam, Esteves et al. (2009) in the UK, Kuleli et al. (2011) in Turkey, Alberico et al. (2012) in Italy, Ellison and Zouh (2012) in Cameroon, Addo et al.

**Table 1** Previous methods of the study area that was used in previous research

Sl. no	Study area	Applied method	References
1	Upstream and downstream of Farakka barrage (the Ganga River)	Manual and traditional polygons superimpose or overlay methods were used for the cross-sectional creation and EA measurement	Thakur et al. (2011)
2	Upstream and downstream of Farakka barrage (the Ganga River)	Traditional and manual methods were used for EA measurement	Das (2011)
3	Upstream and downstream of Farakka barrage (the Ganga River)	Manual and traditional polygons superimpose or overlay methods were used for EA measurement	Sinha and Ghosh (2012)
4	The left bank site of the river Ganges of the Malda district	Manual and traditional polygons superimpose or overlay methods were used for the cross-sectional creation and EA measurement	Mukherjee and Pal (2017)
5	The left bank site of the river Ganges of the Malda district	Manual and traditional polygons superimpose or overlay methods were used for EA measurement	Mondal and Mandal (2018)
6	The Ganga River from Bhagalpur to Lalgola	Manual and traditional polygons superimpose or overlay methods were used for the channel shifting measurement	Pal and Pani (2019)
7	The left bank site of the river Ganges of the Malda district	Traditional and manual methods were used for transects creation and EA calculation	Majumdar and Mandal (2020)
8	The Ganga River from Bhagalpur to Farakka	Manual and traditional polygons superimpose or overlay methods were used for EA measurement	Raj and Singh (2020)
9	The Ganga River from Sahibganj (Jharkhand) to Jalangi (West Bengal)	Traditional and manual methods were used for reach division creation	Ashwini et al. (2020)
10	Upstream and downstream of Farakka barrage (the Ganga River)	Manual and traditional polygons superimpose or overlay methods were used for EA measurement of different blocks boundary	Sarif et al. (2021)

(2008) in Ghana, Natesan et al. (2013), Mukhopadhyay et al. (2012) in India, Rahman et al. (2011) in India and Bangladesh, etc. Generally, the DSAS model is used in the context, particularly for the sea shoreline migration. However, in this study, the right and the left bank can be separately mapped with a higher degree of accuracy (Ashraf and Shakir 2018; Jana 2019; Hasanuzzaman et al. 2022b).

Additionally, we calculated village boundary-wise EA, bank erosion hazard index (BEHI), and river embankment breaching vulnerability index (REBVI) at the left bank buffer. Based on previous literature, governmental reports, and news sources, it is evident that the left bank of the lower Ganga River is facing a precarious situation caused by massive bank erosion. However, our work has been carried out at the village boundary level, as this is where various developmental programs and schemes are implemented through the Panchayat Development Plan by the Ministry of Panchayati Raj and the Ministry of Rural Development, under the Government of India.

The bank erosion hazard index (BEHI) is a useful tool for assessing the risk of bank erosion along riverbanks. It takes into account various factors, including bank height, bankfull height, bank protection, bank combination, vegetation root depth, root density, and bank material stratification, to provide a comprehensive assessment of the bank erosion hazard. The BEHI has been applied in various studies and has been found to be accurate and reliable (Rosgen 2006; Mazzorana et al. 2010; Azamathulla et al. 2015; Cheng et al. 2019; Islam et al. 2020). The BEHI was developed by the US Army Corps of Engineers (USACE) in 1998. The river embankment breaching vulnerability index (REBVI) is a method that helps in identifying areas that are most vulnerable to embankment breaching and prioritizing measures to reduce the risk of damage to infrastructure and communities. The REBVI was applied in various studies (Liu et al. 2021; Wang et al. 2020). The method involves the integration of three vulnerability factors: bank materials and geotechnical attributes, the geometry of embankment, and hydraulic pressure.

However, the scientific automated methods for the calculation of historical and future riverbank EA, village-wise calculation of riverbank EA, calculation of BEHI, and calculation of river embankment breaching are not figured out in the previous studies. It is a big research gap in the study area. Therefore, the main objectives of the study are (1) to measure the past, present and future EA rate of both banks of the study river using the DSAS automated model; (2) to calculate the village-wise EA of the left bank of the study area; and (3) to calculate BEHI and REBVI of the left bank of the study area. Thus, this study will act as a spatial guideline for the administration of riverbank erosion management.

## 2 Study area

The Ganga River is one of the largest rivers in India. As the Ganga River enters West Bengal, it becomes confined on both sides due to the surrounding Diara region on the left bank (Malda) and the outliers of the Rajmahal hills on the right bank. The Diara region is an alluvial deposition area between the upland and the marshy Tal track. According to the Geological Survey of India, along the left bank, there is the Malda–Kishanganj Fault, while along the right bank the Rajmahal Fault exists. Those faults have forced the Ganga River of the study area to flow in a relatively narrow valley (Sinha and Ghosh 2012). During the monsoon, the Ganga River water level crosses the danger or the extreme danger

level. According to the Central Water Commission of India, the average annual sediment load is 200.53 (Mt) at the Farakka (Khan et al. 2018).

Geographical area extended between 24°39'38"N to 25°13'16"N latitude and 87°46'25"E to 88° 00'16"E longitude with covering the distance of 8.7 km (Fig. 1). This portion of the river is very dynamic channel behavior. People are facing every year with

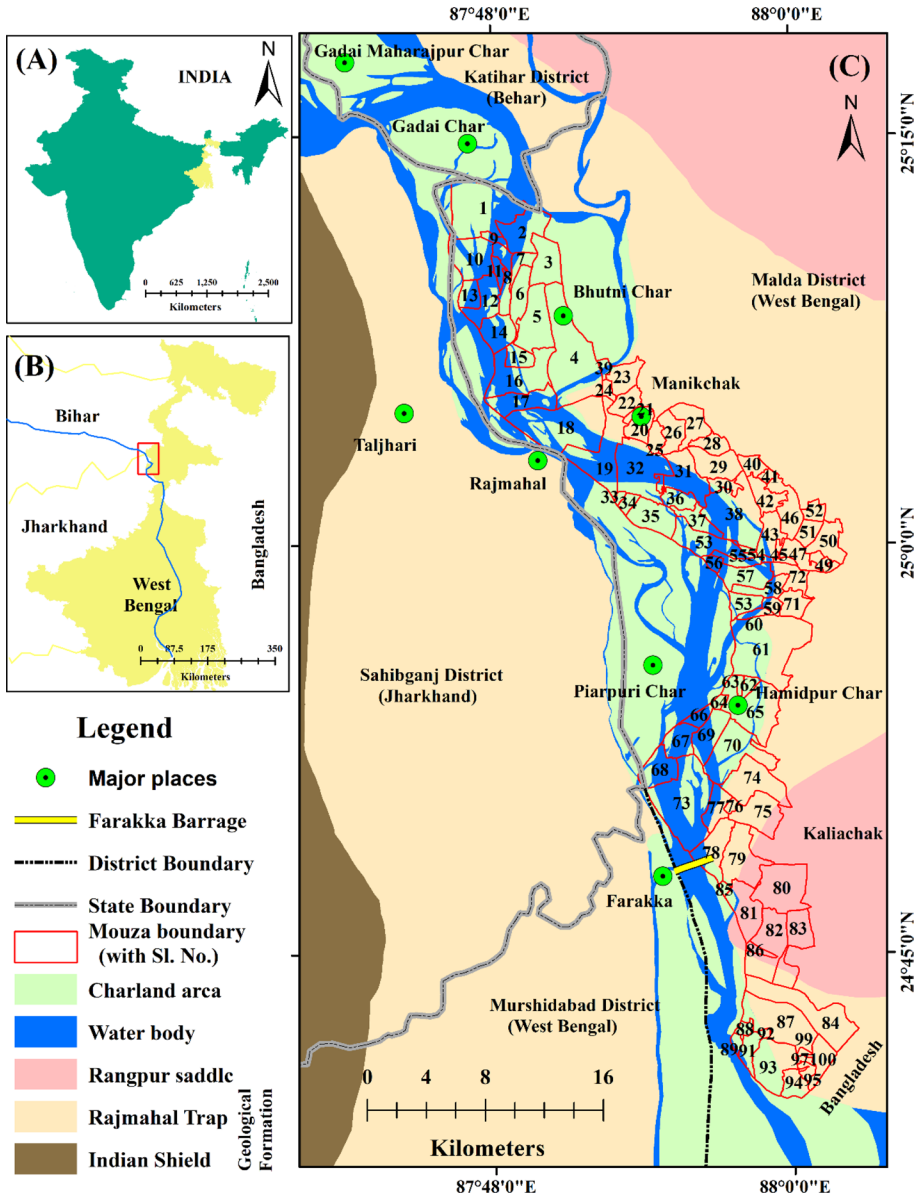


**Fig. 1** Location map of the study area **a** India, **b** West Bengal, **c** the Ganga River floodplain with river buffer mouza/village

natural hazards due to shifting of the river channel, seasonal submergence of *char land* (channel bar) and flooding, etc. The Planning Commission (1996) reported that around 4.5 lakh of people had lost their homes in 40 village panchayats (the village administration system in India) of Malda district, India (Dutta 2011). In this study, transect-wise EA and prediction have been estimated along both the banks; however, mouza (village)-wise EA and prediction have been calculated for only the left bank or the most affected mouzas of the Malda district. The present study has identified 100 mouzas (smallest administrative unit of India for revenue collection) along the left bank of the Ganga River in Malda district (Fig. 1). These 100 villages are distributed in four blocks, i.e., Manikchak block (39 villages), English Bazar (11 villages), Kaliachak-I (23 villages), and Kaliachak-III (27 villages) (ST1).

### 3 Data used

In the research, MSS, TM, ETM+, and OLI datasets used in the years of 1973, 1987, 1997, 2007, and 2020 to demarcate the channel banklines (Table 2). We have selected these above years because of image availability, cloud-free, and ten-year-plus interval. Between November and January have been selected, as the images are clouds-free during this time period. All the satellite images were projected in the UTM projection with zone 45 north and WGS84 datum and resample in the ArcGIS environment. To maintain the data quality, all the images have been co-registered using the first-order polynomial model with the accuracy of root mean square error (RMSE) of less than 0.5 pixels with a minimum number of ground control points (GCPs). We have selected 29 sampling points of left bank of the study area for BEHI and REBVI models. The details of collection data are given in Supplementary Material 1 (SM1). The work has been carried out as per the following methodology (Fig. 2).

#### 3.1 Bankline extraction

We have used the normalized difference water index (NDWI) for bankline extraction based on Eq. 1.

$$\text{NDWI} = \text{Green} - \text{NIR} / \text{Green} + \text{NIR} \quad (1)$$

The value of the NDWI ranges from  $-1$  to  $1$ . Theoretically, NDWI values above  $0$  represent water bodies and NDWI values below  $0$  indicate non-water-body areas (Zheng et al. 2021). We have extracted the river bank buffer area (left and right banks separately) by the polygon feature from the NDWI final images in ArcGIS 8.1 software. After that, we converted the classified images into polygon features and extracted the riverbank lines (de Bethune et al. 1998; Jana 2019). This whole process is completed by automatic techniques. Therefore, this banklines extraction method is more accurate than the traditional digitization method. The digitization method has the chance of human bias because this method human manually digitizes the bankline.

**Table 2** Data type used for different purposes and respective sources

Data type	Specification				Purpose		Sources of data
	Satellite Images	Acquisition date	Path/Row	Spatial resolution (in m)	For bankline extraction		
Secondary data	Landsat-1 MSS	23.11.1973	129/043	60			<a href="http://earthexplorer.usgs.gov">http://earthexplorer.usgs.gov</a>
	Landsat-5 TM	08.12.1987	129/043	30			
	Landsat-5 TM	22.12.1997	129/043	30			
	Landsat-7 ETM	16.01.2007	129/043	30			
	Landsat-8 OLI-TIRS	15.12.2020	129/043	30			
Primary data	Bank height, bank full height, root depth, root density, surface protection, bank angle, soil texture, base width, bank slope, and water weight					For BEHI and REBVI score calculation	Primary survey

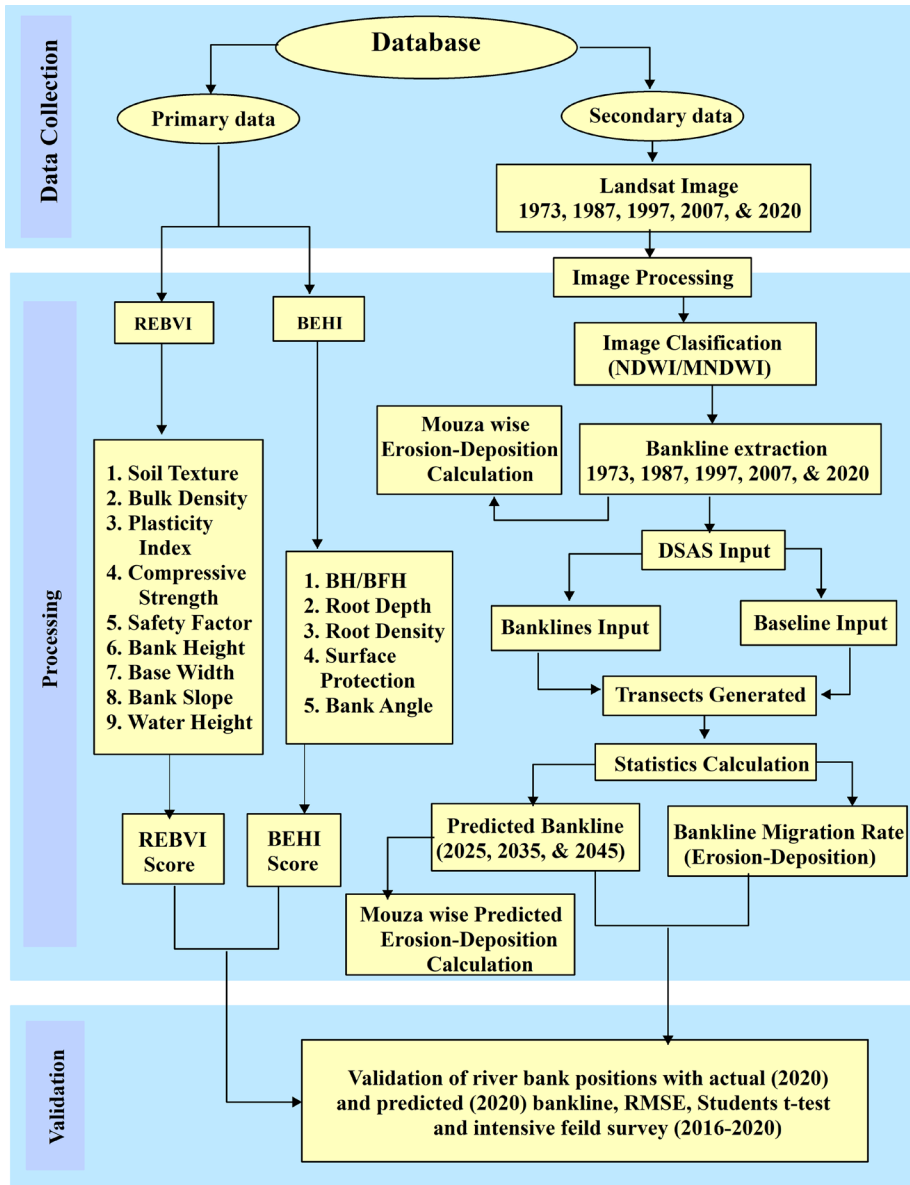


Fig. 2 Conceptual framework of the methods used

### 3.2 Estimation of erosion–accretion (EA) rate and its prediction

In the present work, the DSAS (version 4.3) extension tool of ArcGIS (version 8.1) has been used to assess the rate of EA of the banklines. Subsequently, their predictions have also estimated by using the reference extracted baselines and auto-generated transects.



For the DSAS-based statistical output, two further models have been employed such as end-point rate (EPR) model for computing present EA of the banklines and linear regression (LRR) model to estimate the shifting of future banklines.

### 3.2.1 EPR model for calculating the bankline EA rate

The rate of change in the position of banklines is frequently applied to summarize the historical bankline shifting and their future prediction. The model is based on the assumption that the observed periodical rate of change of bankline position is the best estimate for prediction of the future bankline (Fenster et al. 1993) and no prior knowledge regarding the flow discharge or sediment transport is required because the cumulative effect of all the underlined processes is assumed to be captured in the position history (Li et al. 2001).

In the EPR model, based on the availability of data, the studied time period is divided into four temporal datasets, i.e., 1973 to 1987, 1987 to 1997, 1997 to 2007, and 2007 to 2020 (Fig. 3). For each dataset, superimposed technique has been portrayed to demarcate bankline positions and achieved a final line of overlapping visualization and this line is found out as a superimpose line. Afterward, a buffer of 100 m distance from the superimpose line is used to draw toward the right for the right bank and left for the left bank to demarcate the baselines. Therefore, transects have been placed at a 50-m gap on the baseline. These transects are created at the acute angle to the baseline up to 15 km

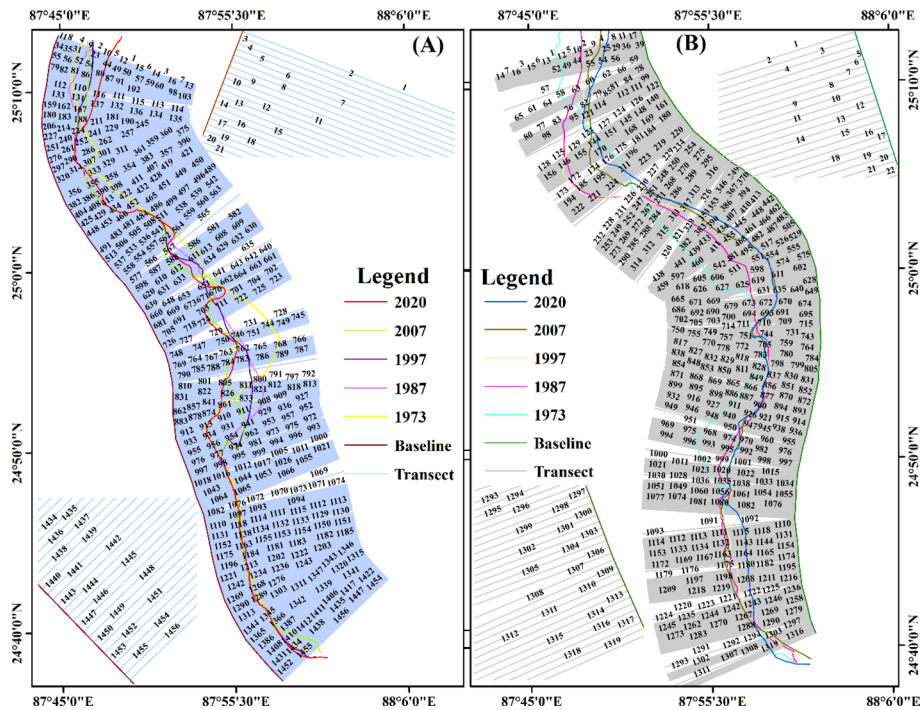


**Fig. 3** Different banklines (1973–2020) are positioned along the baseline. All transects are oriented at angle with the corresponding baselines. **a** Right bankline and **b** left bankline

distance away from both banks. These transects are auto-generated with  $\pm 0.5$  m uncertainties depending on the orientation of the baselines. Moreover, around 1347 transects on the left banks and 1456 on the right bank are placed along the baseline with 50 m spacing to cover the entire selected tracts (about 8.7 km) (Fig. 3).

$$\text{EPR} = \frac{\text{Distance of bankline movement}}{\text{Time between earlier and recent}} \quad (2)$$

In EPR model, previous and recent data of two banklines are needed for this calculation. Moreover, the model uses data of two years at a single time. For example, the model calculates the EA between 1973 and 1987 based on the change, detected between the periods 1973 and 1987. Thereafter, 1987 to 1997, then 1997 to 2007, and finally 2007 to 2020 to calculate the riverbank EA rates depict the shifting trend over periods.

The result of EPR is applied to calculate the rate of bankline migration and understand the EA nature (Mukhopadhyay et al. 2012; Jana 2019). Therefore, we have used the ‘Y’ for positions of the earlier ( $Y_{\text{eb}}$ ) and the recent ( $Y_{\text{rb}}$ ) bankline. In this attempt, it is used as ‘Y’ to denote the projected bankline position which is estimated by the following equation:

$$Y = \alpha_{\text{EPR}} + \beta_{\text{EPR}}X \quad (3)$$

where  $X$  is the time interval ( $X_{\text{eb}} - X_{\text{rb}}$ ) between earlier bankline ( $X_{\text{eb}}$ ) and recent bankline ( $X_{\text{rb}}$ ),  $\alpha_{\text{EPR}}$  is the model intercept, and  $\beta_{\text{EPR}}$  denotes the rate of riverbank shifting (slope or regression coefficient).

On the other hand, EPR intercept is calculated by Eq. 4.

$$\alpha_{\text{EPR}} = Y_{\text{eb}} - \left\{ \frac{Y_{\text{eb}} - Y_{\text{rb}}}{X_{\text{rb}} - X_{\text{eb}}} \right\} X_{\text{eb}} = Y_{\text{rb}} - \left\{ \frac{Y_{\text{eb}} - Y_{\text{rb}}}{X_{\text{rb}} - X_{\text{eb}}} \right\} X_{\text{rb}} \quad (4)$$

The rate of bankline migration for a given set of transects,  $\beta_{\text{EPR}}$ , is calculated by Eq. 5:

$$\beta_{\text{EPR}} = \left\{ \frac{Y_{\text{eb}} - Y_{\text{rb}}}{X_{\text{rb}} - X_{\text{eb}}} \right\} \quad (5)$$

### 3.2.2 LRR model for predicting the bankline erosion–accretion/shifting rate

LRR model uses statistics of model generated baseline, which is demarcated by temporal period of bankline migration. It has shown bank position of the subsequent year of the selected time span. Therefore, the channel side position of the dataset 2020 is considered as a common baseline to all sets. The result of this attempt has been scrutinized by the least-square method (fitting a regression line) to predict the channel shifting and bankline position (Thieler et al. 2009). For this, a regression line is placed to all linear series, points along a user particular transect. Afterward, the river bankline migration rate is estimated by fitting the least-square regression lines. This process was used for all selected bankline of a particular transect. Therefore, this method is used for predicting the position. The short-term (2025), intermediate-term (2035), and long-term (2045) basis with a period of 5 years, 15 years and 25 years, respectively, were used for prediction in this study. Moreover, position of bankline of 2020 was predicted for accuracy assessment.

Then, the value of EPR is used to predict the future riverbank positions ( $Y_{pb}$ ). This is because the predicted riverbank position ( $X_{pb}$ ) can extend beyond the recent riverbank (either at left or at right). Hence, Eq. 5 is modified and formulated through LRR by Eq. 6.

$$Y_{pb} = \{ \beta_{EPR} (X_{cb} - X_{rb}) \} + Y_{rb} \tag{6}$$

### 3.3 Determination for village-wise EA area

In this study, we also compared the bankline position of the river concerning selected different datasets. After that, we calculated the EA rate separately for each period in the selected village boundaries at the left bank. Therefore, village/mouza-wise EA was manually calculated with the help of ArcGIS (version 8.1) software.

### 3.4 BEHI measurement

BEHI is an important fluvial geomorphic tool for the analysis of the susceptibility of riverbank erosion (Rosgen 2006). The BEHI methodology evaluates the function of some erodibility variables including bank height, bankfull height, bank protection, bank combination, vegetation root depth, root density, and bank material stratification. As per the guidelines of Rosgen (2001, 2006) (Table 3), BEHI score has been calculated. All collected primary data of 29 samples of the left bank (facing downstream) by the field survey have been used for BEHI score calculation (Simpson et al. 2014; Ghosh et al. 2016) (SM 2).

### 3.5 Calculation of REBVI

We have measured 29 samples of riverbank properties for calculation of REBVI score (Mondal et al. 2012). Detailed observations of breach parameters such as bank materials and geotechnical attributes (soil texture, bulk density, plasticity index, compressive strength, and safety factor), the geometry of embankment (bank top height, base width, and bank slope), and hydraulic pressure (water height) have been investigated.

The embankments breaching has been calculated to a multi-criteria approach for all of the input variables. We have utilized weighting systems based on the values from 0 to 4, where ‘4’ means very highly vulnerable, ‘3’ highly vulnerable, ‘2’ moderately vulnerable, ‘1’ less vulnerable, and ‘0’ very less vulnerable. Therefore, based on their importance and stability of materials to the potential of embankments breaching a set of continuous data have ranks from 1 to 5. The ranks assigned to different features of the individual themes are presented in Table S2. After deriving the normal weights and ranks, all individual parameters have been integrated in a linear model to determine REBVI using Eq. 7.

$$REBVI = (R_{ST} \times W_{ST}) + (R_{BD} \times W_{BD}) + (R_{SF} \times W_{SF}) + (R_{TH} \times W_{TH}) + (R_{BS} \times W_{BS})(R_{WH} \times W_{WH}) \tag{7}$$

where  $R$ =rank value,  $W$ =weight value,  $ST$ =soil texture,  $BD$ =bulk density,  $SF$ =safety factor,  $TH$ =top height,  $BW$ =base width of embankment,  $BS$ =bank slope, and  $WH$ =water height (SM3).

**Table 3** Guidelines for measuring complete BEHI (after, Rosgen 2001)

BEHI category	Bank height/ Bankfull height	BH/BFH Score	Root depth (% of BFH)	Root depth Score	Root density/ BH (%)	Root density/ BH Score	Surface protection (Avg. %)	Surface protection Score	Bank angle (°)	Bank Angle Score	Total Score, by category
Very low	1.0–1.1	1.45	90–100	1.45	80–100	1.45	80–100	1.45	0–20	1.45	≤ 7.25
Low	1.11–1.19	2.95	50–89	2.95	55–79	2.95	55–79	2.95	21–60	2.95	7.26–14.75
Moderate	1.2–1.5	4.95	30–49	4.95	30–54	4.95	30–54	4.95	61–80	4.95	14.76–24.75
High	1.6–2.0	6.95	15–29	6.95	15–29	6.95	15–29	6.95	81–90	6.95	24.76–34.75
Very high	2.1–2.8	8.5	5–14	8.5	5–14	8.5	10–14	8.5	91–119	8.5	34.76–42.50
Extreme	> 2.8	10	< 5	10	< 5	10	< 10	10	> 119	10	42.51–50

### 3.6 Model validation methods

DSAS model has been used for estimating the future riverbank EA and future bankline position. But before the future prediction, the model has to be validated with the current circumstances (Mukhopadhyay et al. 2012; Jana 2019). Therefore, the LRR method is employed to predict future bankline position based on EPR (slope), interval, and intercept value. Based on this, the estimated bankline position of 2020 is calculated and the predicted bankline is verified with the actual bankline 2020. It is demarcated from the satellite image of 2020. The positional error is estimated using RMSE. It is carried out using Eq. 8.

$$\text{RMSE} = \left[ n^{-1} \sum_{i=0}^n (X_{\text{mb}} - X_{\text{ab}})^2 + (Y_{\text{mb}} - Y_{\text{ab}})^2 \right]^{1/2} \quad (8)$$

where  $X_{\text{mb}}$  and  $Y_{\text{mb}}$  are the model estimated bankline and  $X_{\text{ab}}$  and  $Y_{\text{ab}}$  are the actual bankline in  $X$  (time) and  $Y$  (position) coordinates the sample points, respectively.

Potential errors are associated with satellite maps (datum changes, different surveying standards, projection errors, distortions from uneven shrinkage, etc.) (Anders and Byrnes 1991). In the work, four type errors are identified for measuring the rate change, and it may be of both position- and calculation-related errors. Calculation uncertainties are related to the skill and approach such as pixel error  $E_p$ , digitizing error  $E_d$ , and rectification error  $E_r$ , and positional uncertainties are related to the features and phenomena that reduce the precision and accuracy of defining a bankline (both) position from a given dataset such as seasonal error  $E_s$  (Kankara et al. 2015). Finally, total uncertainty value was estimated for each bankline by accounting both positional and measurement uncertainties as:

$$Et = \pm \sqrt{E_p + E_d + E_r + E_s} \quad (9)$$

The bankline positional error is also verified with 100 GCPs collected from the field survey during 2019–2020. Out of these, GCPs and 29 GCPs have been used for BEHI and REBVI calculation. The RMSE and t-test are adopted for the model validation of estimated banklines (left and right), which gives an accurate portrayal between actual and predicted banklines.

## 4 Results

### 4.1 DSAS-based riverbank EA and future prediction assessment

The DSAS model-based transect-wise riverbank EA trend is illustrated in Table 4 and Fig. 4. The result from 1973 to 1987 depicts that the mean erosion rate was 0.129 km/year at the left bank and 0.61 km/year at the right bank. Among the transects, 661 at the left bank and 548 at the right bank were erosion-dominant transects. The EA rate and the number of the affected transect indicated that the channel was very active through the erosion process of both sides of the banks. Therefore, the correspondence of high erosion at both banks indicated channel widening.

During 2007–2020, the mean erosion rate of the left bank was 0.168 km/year and mean erosion rate of the right bank was 0.079 km/year. Among the transects, 455 at the left bank and 296 at the right bank were erosion-dominant transects (Fig. 5). In this observation, the

**Table 4** DSAS model-based mean and standard deviation of erosion–accretion of both bank

Years	Left bank						Right Bank							
	Erosion in km/year		Accretion in km/year		NET	NAT	NST	Erosion in km/year		Accretion in km/year		NET	NAT	NST
	Mean	SD	Mean	SD				Mean	SD	Mean	SD			
1973–1987	0.129	0.082	0.104	0.121	661	357	329	0.061	0.066	0.119	0.123	548	382	526
1987–1997	0.072	0.064	0.020	0.018	484	474	389	0.019	0.030	0.061	0.062	394	462	600
1997–2007	0.106	0.099	0.037	0.029	481	428	438	0.049	0.067	0.026	0.046	442	459	555
2007–2020	0.168	0.139	0.021	0.024	455	494	398	0.079	0.111	0.056	0.051	296	757	403
2020–2025	0.089	0.047	0.032	0.019	473	434	440	0.045	0.040	0.060	0.063	313	544	599
2020–2035	0.151	0.141	0.019	0.018	506	477	364	0.043	0.049	0.026	0.025	318	616	522
2020–2045	0.164	0.149	0.021	0.011	597	438	312	0.031	0.035	0.045	0.041	417	474	565

SD standard deviation, NET number of erosion transects, NAT number of accretion transects, NST number of stable transects

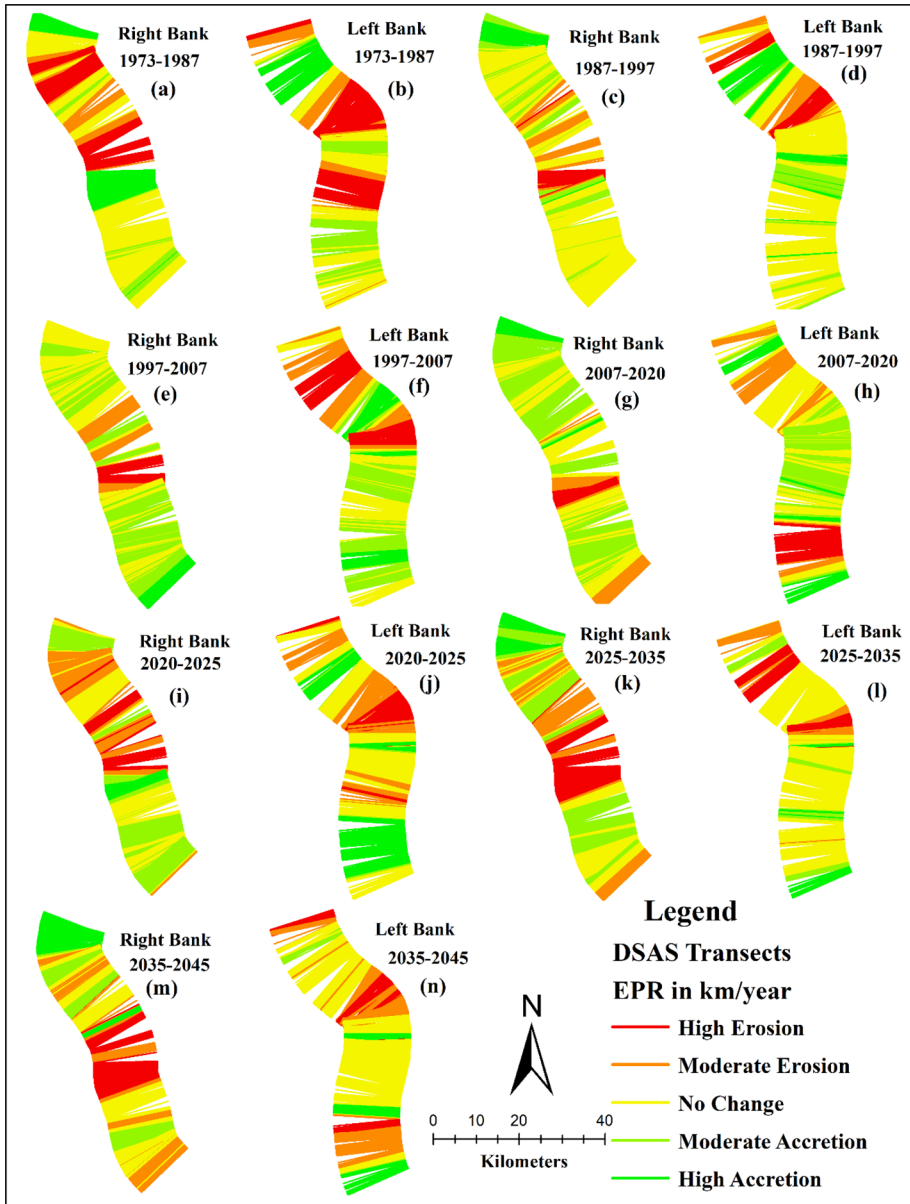


**Fig. 4** DSAS model-based prediction of riverbank erosion and deposition rate along transects during the different study periods, at the both banks. **a** Right bank and **b** left bank of 1973–1987; **c** right bank and **d** left bank of 1987–1997; **e** right bank and **f** left bank of 1997–2007; **g** right bank and **h** left bank of 2007–2020; **i** right bank and **j** left bank of 2000–2025; **k** right bank and **l** left bank of 2025–2035; **m** right bank and **n** left bank of 2035–2045

left bank experiences extensive erosion and disproportionate sediment accretion along the right bank. This result indicates a widening river course triggered by persistent erosion on both banks; as an overall result, the river channel shifts toward the left bank with a large

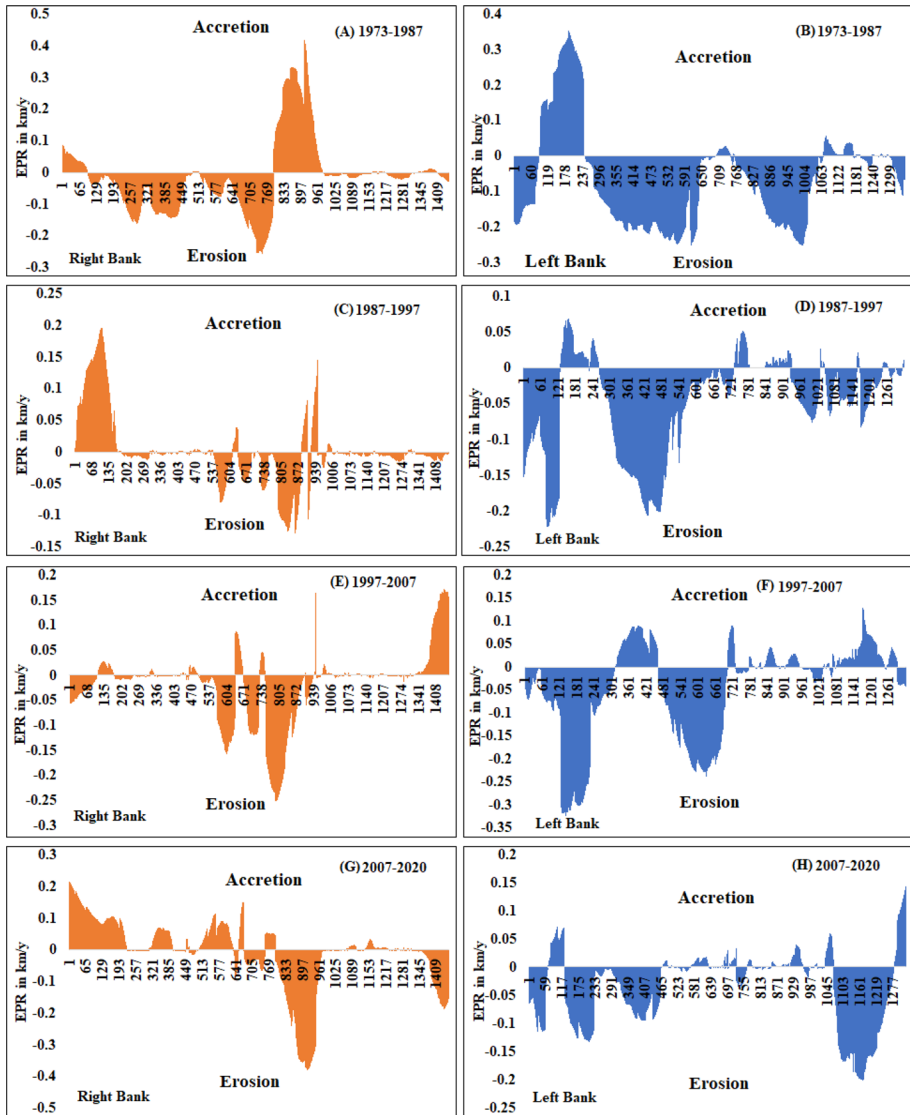


**Fig. 5** DSAS model-based prediction of riverbank accretion–erosion rate during the study periods at the both banks. **a** Right bank and **b** left bank of 1973–1987; **c** right bank and **d** left bank of 1987–1997; **e** right bank and **f** left bank of 1997–2007; **g** right bank and **h** left bank of 2007–2020; **i** right bank and **j** left bank of 1973–2020; **k** right bank and **l** left bank of 2020–2025; **m** right bank and **n** left bank of 2025–2035; **o** right bank and **p** left bank of 2035–2045

extent of sedimentation at the right bank. Also, we observed that from 1973 to the present time bank erosion of left bank is concentrated pocket places from all over banklines. In recent times, erosion of the left bank has consented lower part of the study area.





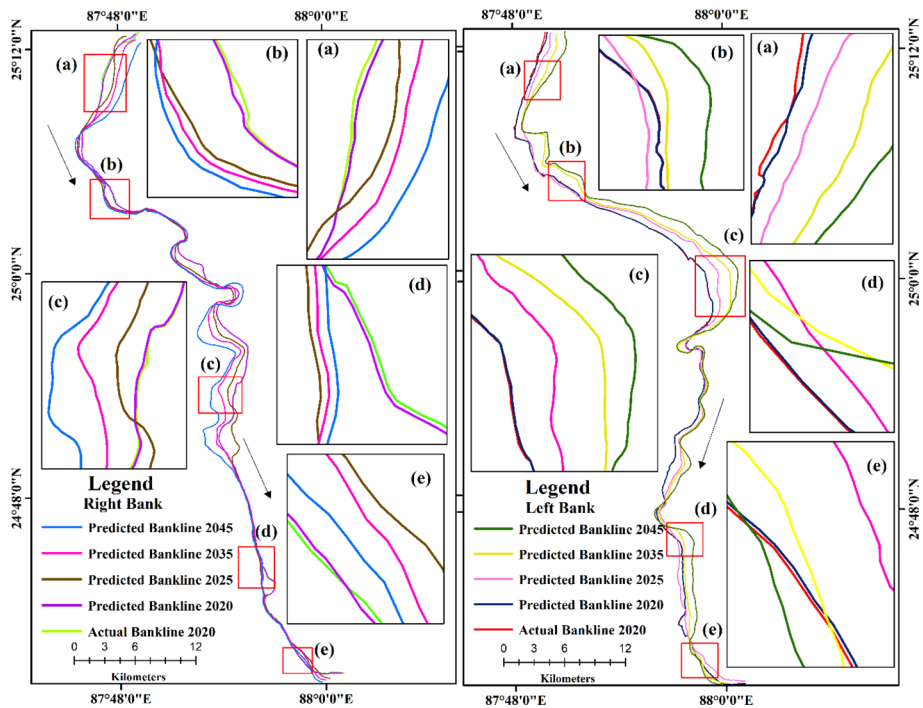


**Fig. 6** Spatial pattern of bankline migration after prediction in the years 2020, 2025, 2035, and 2045

process will likely dominate the left bank of the riverbank shifting through EA in future (Fig. 6).

#### 4.2 Village-wise spatial distributions of erosion–accretion and future prediction analysis

This study provides a detailed portrayal of the spatial distributions of erosion and accretion across 100 villages located in the buffer zone of the Ganga River, specifically the adjacent village areas of Malda district, during the period of 1973–2045 (Fig. 7). The overall results of the study indicate that regular erosion was observed in 13 villages, while three villages experienced consistent accretion throughout the entire study period. From 1973 to 2020, the Palgachhi, Jagannathpur, Gadai, Narayanpur, Manikchak, and Gopalpur villages become the most eroded or vulnerable villages. During the predicted period from 2020 to 2045, 21 villages will show active erosion in this vulnerable villages in future.

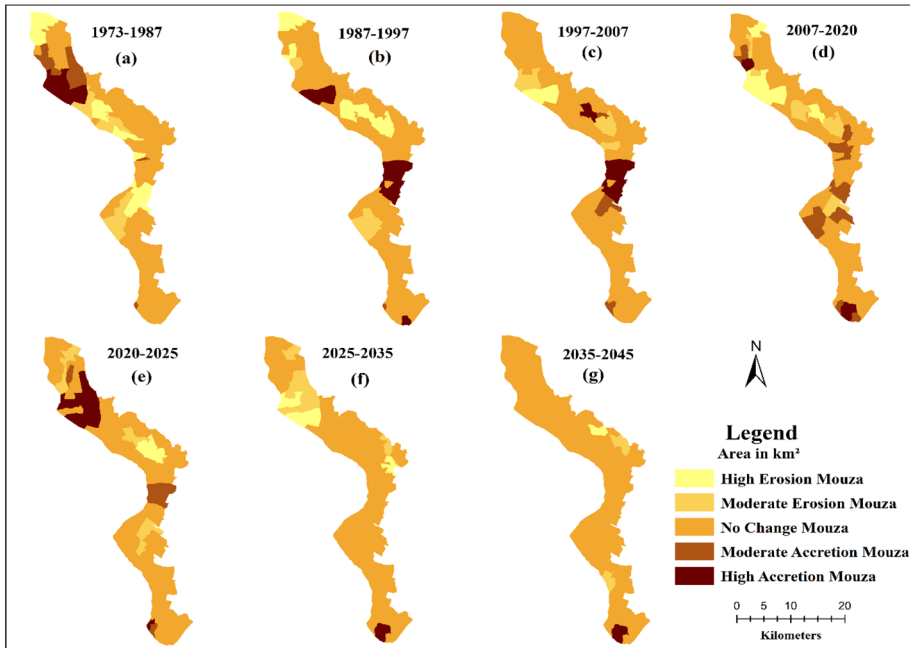


**Fig. 7** Spatial distributions of erosion and deposition area at the left bank buffer mouza/villages during the periods **a** 1973–1987, **b** 1987–1997, **c** 1997–2007, **d** 2007–2020, **e** 2020–2025, **f** 2025–2035, and **g** 2035–2045

**Table 5** DSAS model-based results of RMSE and Student’s t-test

Transects number	Bankline position (Actual 2020 and predicted 2020)	RMSE	( $p < 0.05$ ) Two-tail
0–336	Left bank	0.192	0.114
0–364	Right bank	0.124	0.129
337–673	Left bank	0.131	0.165
365–728	Right bank	0.247	0.236
674–1009	Left bank	0.211	0.203
729–1092	Right bank	0.171	0.209
1010–1347	Left bank	0.139	0.019
1093–1456	Right bank	0.103	0.208

### 4.3 Model validation

The linear regression rate (LRR) was 2.4 m/y (left bank) and 2.2 m/y (right bank) for all transects. The band of confidence around the reported rate of change was  $-2.6 \pm 0.78$ . Therefore, it can be 88% confident that the true rate of change is between 3.21 and 1.79 m/year. Also,  $R^2$  (0.82 for the left bank and 0.79 for the right bank) value justified the acceptance of the work (Supplementary Fig. 1). Therefore, the riverbank uncertainty was sated at 5 m at both banks during the model run. The RMSE at each

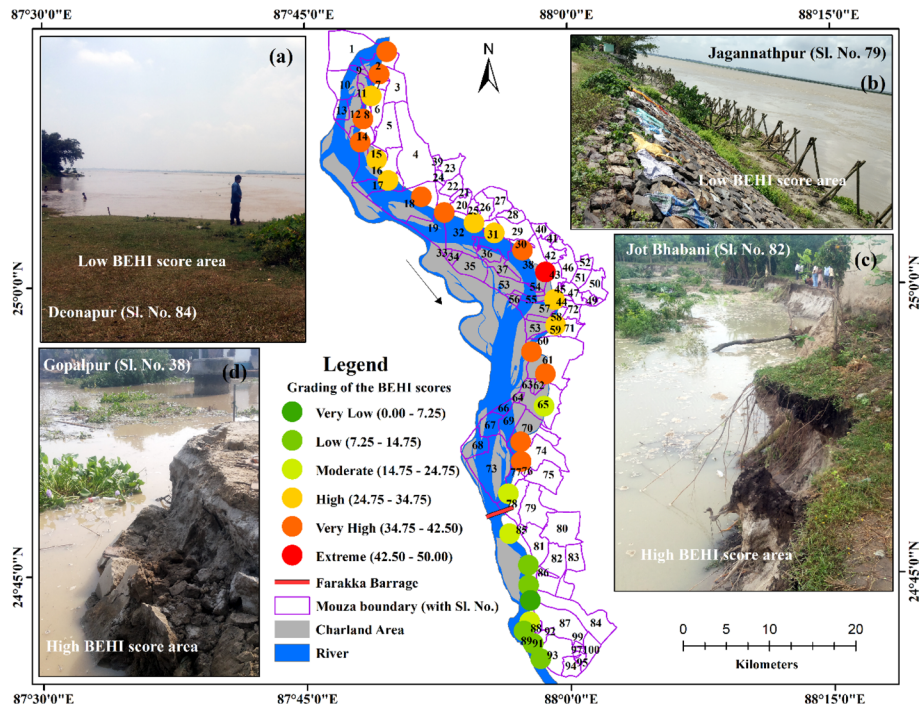


**Fig. 8** Sample segment (location)-specific mean BEHI ratings along the left bank of the Ganga River, **a** low BEHI score area (7.25) at Deonapur, **b** low BEHI score area (22.75) at Jagannathpur, **c** high BEHI score area (42.45) at Jot Bhabani, **d** high BEHI score area (43.95) at Gopalpur

transect point was placed by error vectors, and the BS varies from 0.103 to 0.247 with an overall mean error of 0.165 (Table 5). The t-test results reveal that the model has a good prediction capacity ( $p < 0.05$ ). Therefore, this result was accurately matched with the predicted bankline position corresponding with the actual bankline position (Fig. 6).

#### 4.4 BEHI assessment

The selected variables of 29 samples used for BEHI scores were rated, and based on these ratings, an erosion hazard value map for the left bank has been created (Fig. 8). The findings indicate that out of the 29 sample segments analyzed, 14 were deemed to be at a very high to extremely vulnerable level of bank erosion hazard due to toe erosion caused by helical flow. Consequently, these villages were identified as highly dynamic erosional areas in the study. In contrast, five segments were rated as having low to very low vulnerability to bank erosion hazard, which can be attributed to factors such as low slope, sedimentation, and the presence of riparian vegetation, as well as engineering constructions such as embankments and spurs. In this analysis, we observed that in the upper part of the Farakka barrage, BEHI value was high to the extreme, but at the lower stretch of the Farakka barrage, BEHI value was low to very low (ST3). The values of bankfull height were very high

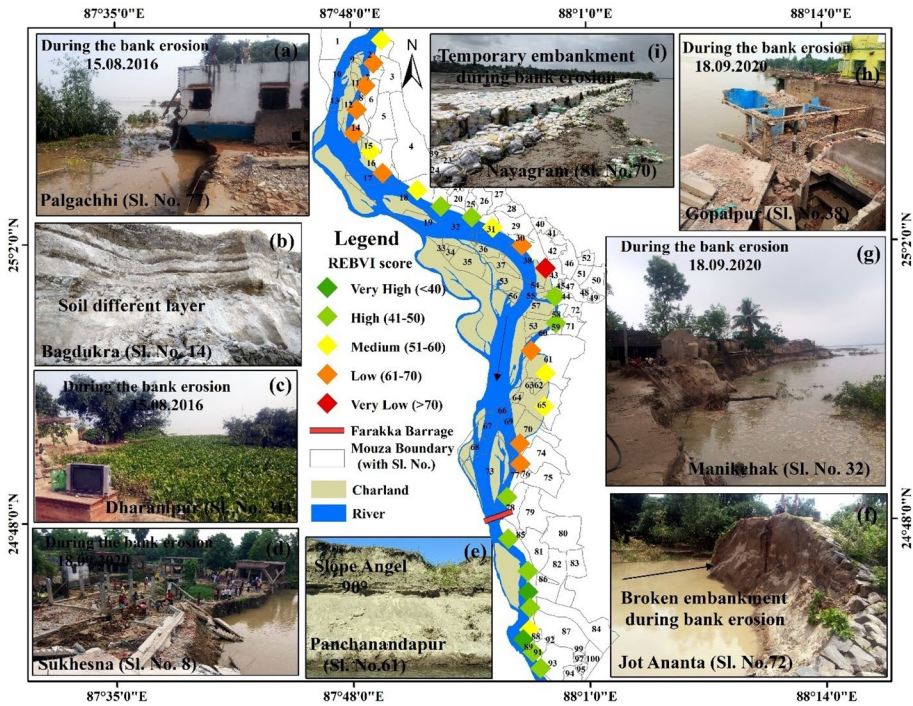


**Fig. 9** Sample segment (location)-specific mean REBVI ratings along the left bank of the Ganga River, **a** during the bank erosion time at Palgachhi mouza, **b** during the bank erosion time at Dharampur, **c** during the bank erosion time at Manikchak, **d** during the bank erosion time at Gupalpur, **e** during the bank erosion time at Sukhesna, **f** above 90° angle slope at Panchanandapur, **g** soil different layers at Bagdukra, **h** temporary embankment at Nayagram, **i** broken embankment at Jot Ananta

in most of the bank segments of the upper part of the Farakka barrage because the water levels rise significantly during peak monsoon season.

### 4.5 REBVI assessment

The REBVI outcome of selected variable of 29 samples depicted that highest score was less potential for the embankment breaching or riverbank erosion (Table 8). The REBVI score was distributed across five categories, namely very high (a score of less than 40 indicates the high potential to prevent embankment breaching and ensure slope stability), high (scores ranging from 41 to 50), medium (51–60), low (61–70), and very low (scores greater than 70 indicate a very high probability of embankment breaching due to bank failure, piping, and overtopping). According to the REBVI score, Suzapur Mandai (S24) and Par Paranpara (S27) were the potential to prevent riverbank erosion and potential for slope stability. Gopalpur (S13) was a very high probability of riverbank erosion due to bank failure, piping, and overtopping (Fig. 9). Also, nine sample segments have a high probability of embankment breaching (ST4).

## 5 Discussion

The lower part of the Ganga River has been facing high channel shifting and high bank EA almost every year and continuously changed its buffer areas with time. Our study findings are supported by the works of Ashraf and Shakir (2018) and Jana (2019) where they have clearly demonstrated the role of the DSAS model rather than traditional approaches. However, in riverbank erosion, such automated DSAS models are rare in the study regions. Our study attempted to foster a scientific calculation of erosion risk in the context of massive riverbank erosion of the Ganga River which is unknown in the previous attempts (Pal and Pani 2019; Majumdar and Mandal 2020; Raj and Singh 2020; Ashwini et al. 2020; Sarif et al. 2021). The present study indicates that the Ganga River study area displayed high levels of erosion activity on its left bank while demonstrating significant accretion activity on its right bank. The DSAS-based prediction suggests that the same trends observed in the present analysis will persist into the future. Furthermore, our observations indicate that the upper part of the Farakka barrage is the most dynamic channel, which is evidenced by frequent migration. In contrast, the lower section of the barrage displays relatively stable and sequential movement along the left bank. Over the past 47 years, the course of the Ganga River has undergone a significant and highly dynamic adjustment to meet its evolving needs. However, this change in channel behavior has occurred in a dramatic and potentially dangerous manner, highlighting the need for a thorough assessment. Nonetheless, the process of understanding the underlying causes and implications of these changes is exceedingly complex.

The river Ganga changes its bank morphology and land utilization practices along river bank adjacent area during the monsoon period (from June to September). According to Singh et al. (2007), after the Farakka barrage construction (1971) flood frequency is rapidly increased. In 1998, extreme floods occurred that has caused the highest water level ever for the study area which was recorded at 25.40 m (District Human Development Report: Malda, West Bengal, 2007). For the study part of the Ganga River, it is observed that erosivity of water is affected by the amount of discharge and fluctuation in the river regime of the Ganga River which in turn induces bank erosion by various mechanisms, especially by piping action (Rudra 2010; Thakur et al. 2011). Thus, in the Ganga and the Fulahar rivers, the danger level is 24.69 m to 27.43 m and the extreme danger level is 25.30 m to 28.35 m (Flood Forecasting Cell, Irrigation Division, Malda, 2010) (Fig. 10).

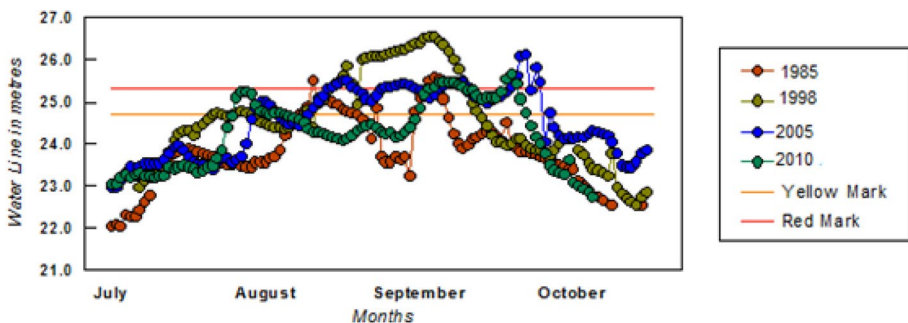


**Fig. 10** River flow characteristics during the monsoon at Farakka 1985–2010 (the yellow mark denotes the danger water level and red mark denotes the extreme danger water level) (Source: Flood Forecasting Cell, Irrigation Division, Malda, 2010)

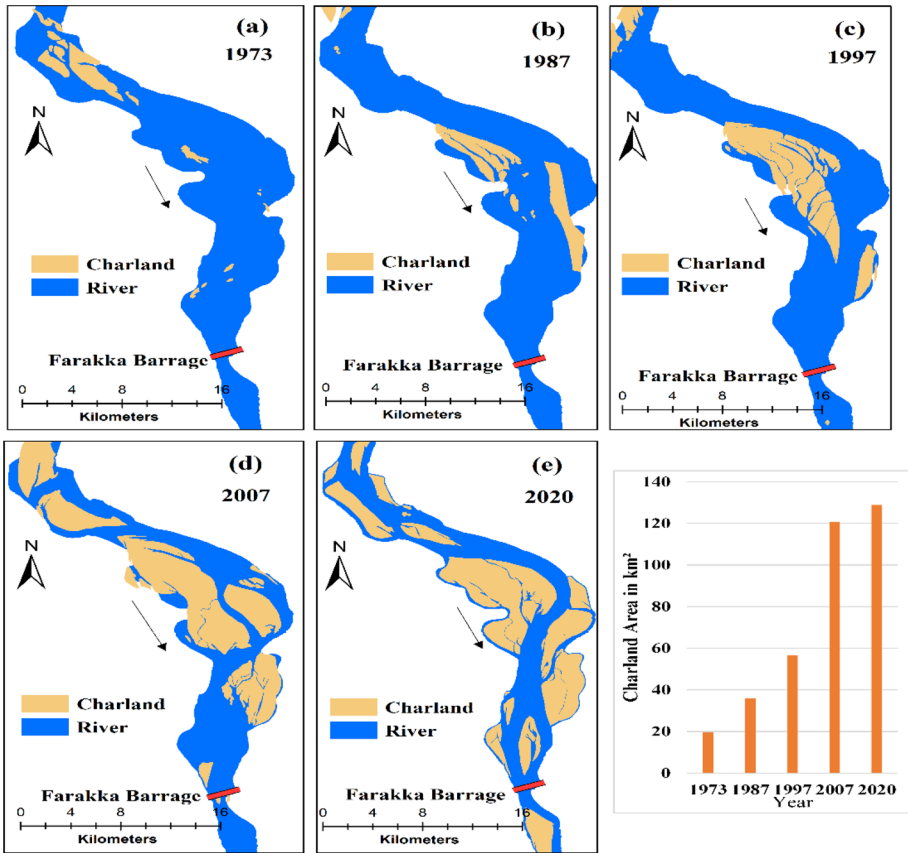


Fig. 11 Charland area extension of the study area, a 1973, b 1987, c 1997, d 2007, e 2020

At this time, the high discharge of water forcefully hits the river banks and the bank of the river to collapse due to the imbalanced pressure. This part of the Ganga River has possibly been changed due to the construction of the Farakka barrage that asserts exclusively to the continuous aggradations sand and gravel bar formation. Sediment supply and its deposition under fluctuating discharge disturb the morphology of a river (Bandyopadhyay et al. 2014) and lead to entropy maximization that induces instability. Moreover, we have calculated charland (deposited inland bar) area of the study area which depicts that charland area has gradually increased during the study time period. During the last 47 years (1973–2020), the total charland accretion is 362.06 km<sup>2</sup> and the annual charland accretion rate is 7.70 km<sup>2</sup>/y (Fig. 11). This huge sediment load in the monsoon period has a significant impact on channel instability in this study area.

However, this work provided a dataset of the village-wise EA of the river Ganga buffer area in Malda district. Previous works have failed to provide village-wise erosion data, and even governmental data remain unavailable, despite their crucial importance in scientific management. This lack of data represents a significant gap in our understanding of erosion patterns and limits our ability to develop effective management strategies. In the study, six

villages were very vulnerable villages for severe erosion. Besides, 21 villages will be noted as highly vulnerable villages in future.

Erosion and accretion are closely related to BEHI and REBVI. The BEHI assesses the likelihood and magnitude of bank erosion by considering factors such as soil type, vegetation cover, and bank height. BEHI helps to identify areas that are vulnerable to bank erosion and prioritize the implementation of appropriate conservation measures. On the other hand, the REBVI evaluates the vulnerability of river embankments to failure and breaching, which can lead to severe erosion and accretion. REBVI considers various factors such as bank materials, geotechnical attributes, the geometry of embankment, and hydraulic pressure to assess the likelihood of embankment failure. The results of both indices can inform the selection and implementation of appropriate conservation strategies to mitigate erosion and accretion, such as the installation of hard or soft engineering structures or sustainable land-use practices. During our investigation, we noted that in the upper part of the Farakka barrage, both BEHI and REBVI values were observed to be extremely high, whereas in the lower stretch of the Farakka barrage, BEHI and REBVI values were found to be low to very low. Furthermore, we discovered a very high rate of erosion in the upper part of the Farakka barrage, which highlights the need for further investigation and management strategies in this area. Therefore, understanding the relationship between erosion and accretion with BEHI and REBVI is essential for effective management of riverine environments and communities.

Riverbank erosion is a significant threat to riverine communities, infrastructure, and the environment. Therefore, various conservation strategies have been developed to manage this issue, including vegetative bioengineering, hard and soft engineering structures, and sustainable land-use practices. However, implementing these strategies presents various challenges, such as the lack of long-term effectiveness, financial constraints, and limited stakeholder involvement. Additionally, future challenges include the increasing frequency and severity of extreme weather events due to climate change, which can exacerbate riverbank erosion. As a result, there is a need for a continuous research and development of innovative conservation strategies, stakeholder engagement, and policy changes to ensure the long-term sustainability of riverine ecosystems and communities.

## 6 Conclusion

The study findings provide important insights into the riverbank EA rates of the lower part of the Ganga River. The study's predictions of the EA rates using the DSAS model and the calculation of the village-wise EA are also significant contributions to the study. Moreover, BEHI and REBVI calculation of the left bank is a crucial contribution to the understanding of the nature of embankment and riverbank. The results indicated that both banks of the river were highly dynamic from 1973 to 2020 through the EA process, but the left bank was more active than the right bank. Moreover, the erosion process is predicted to dominate the left bank in future. The prediction result reveals the very highly vulnerable condition of 06 villages and 21 villages for highly vulnerable due to left bank erosion. During our investigation, we noted that in the upper part of the Farakka barrage, both BEHI and



REBVI values were observed to be extremely high, whereas in the lower stretch of the Farakka barrage, BEHI and REBVI values were found to be low to very low. The study also validated the DSAS model's accuracy, indicating its acceptance for the work.

During this research, we encountered several challenges, such as the lack of actual village-wise social and physical data, river discharge data, river siltation data, and river cross-profile data. Additionally, we noted the absence of governmental management reports that would contribute to a better understanding of bank erosion and vulnerability. The study presents critical insights that can assist decision makers in prioritizing vulnerable villages and implementing policies and programs aimed at attaining sustainable management while minimizing the effect of future riverbank erosion on the local population. The research underscores the pressing requirement for policy alterations and sustainable development initiatives in the study region, emphasizing the need for prompt action to address the issue of riverbank erosion. To ensure the long-term effectiveness of the proposed recommendations for reducing riverbank erosion, future research must concentrate on examining the potential impact of social programs, infrastructure development, and sustainable management plans on the lower Ganga River and its environs.

**Supplementary Information** The online version contains supplementary material available at <https://doi.org/10.1007/s11069-023-06044-4>.

## References

- Addo KA, Walkden M, Mills JT (2008) Detection, measurement and prediction of shoreline recession in Accra, Ghana. *ISPRS J Photogramm Remote Sens* 63(5):543–558. <https://doi.org/10.1016/j.isprsjprs.2008.04.001>
- Alberico I, Amato V, Aucelli PPC, D'Argenio B, Paola GDI, Pappone G (2012) Historical shoreline change of the Sele Plain (Southern Italy): the 1870–2009 time window. *J Coast Res* 28:1638–1647
- Anders FJ, Byrnes MR (1991) Accuracy of shoreline change rates as determined from maps and aerial photographs. *Shore Beach* 59:17–26
- Ashwini K, Pathan S, Singh A (2020) Understanding planform dynamics of the Ganga River in eastern part of India. *Spat Inf Res* 29(4):507–518. <https://doi.org/10.1007/s41324-020-00373-3>
- Azamathulla HM, Shirazi SM, Ghani AA (2015) Bank erosion hazard index (BEHI) model for Pahang River, Malaysia. *J Hydrol* 529:1203–1212
- Bandyopadhyay S, Ghosh K, De SK (2014) A proposed method of bank erosion vulnerability zonation and its application on the River Haora, Tripura, India. *Geomorphology* 224:111–121. <https://doi.org/10.1016/j.geomorph.2014.07.018>
- Bera B, Bhattacharjee S, Roy C (2019) Estimating stream piracy in the lower ganga plain of a quaternary geological site in West Bengal, India applying sedimentological bank facies, log and geospatial techniques. *Curr Sci* 117(4):662. <https://doi.org/10.18520/cs/v117/i4/662-671>
- Cheng Y, Li L, Li Z, Guo L (2019) Bank erosion hazard assessment along the Xiangjiang River, China. *J Hydrol* 572:647–657
- Das B (2011) Stakeholders' perception in identification of river bank erosion hazard: a case study. *Nat Hazards* 58(3):905–928. <https://doi.org/10.1007/s11069-010-9698-z>
- Das R, Samanta G (2022) Impact of floods and river-bank erosion on the riverine people in Manikchak Block of Malda District, West Bengal. *Environ Dev Sustain* 1–23
- de Bethune S, Muller F, Donnay JP (1998) Fusion of multispectral and panchromatic images by local mean and variance matching filtering techniques. *Fusion Earth Data* 28–30
- Dewan A, Corner R, Saleem A, Rahman MM, Haider MR, Rahman MM, Sarker MH (2017) Assessing channel changes of the Ganges-Padma River system in Bangladesh using Landsat and hydrological data. *Geomorphology* 276:257–279. <https://doi.org/10.1016/j.geomorph.2016.10.017>


- Dutta P (2011) Migration as source of risk-aversion among the environmental Eefugees: the case of women displaced by Erosion of the River Ganga in the Malda District of West Bengal, India, Bielefeld: COMCAD
- Ellison JC, Zouh I (2012) Vulnerability to climate change of mangroves: Assessment from Cameroon, Central Africa. *Biology* 1:617–638
- Esteves LS, Williams JJ, Nock A, Lymbery G (2009) Quantifying shoreline changes along the Sifton coast (UK) and the implications for research-informed coastal management. *J Coast Res* 56:602–606
- Fenster M, Dolan R, Elder J (1993) A new method for predicting shoreline positions from historical data. *J Coast Res* 9:147–171
- Ghosh KG, Pal S, Mukhopadhyay S (2016) Validation of BANCS model for assessing stream bank erosion hazard potential (SBEHP) in Bakreshwar River of Rarh region, Eastern India. *Model Earth Syst Environ* 2:1–15. <https://doi.org/10.1007/s40808-016-0172-0>
- Guchhait SK, Islam A, Ghosh S, Das BC, Maji NK (2016) Role of hydrological regime and floodplain sediments in channel instability of the Bhagirathi River, Ganga-Brahmaputra Delta, India. *Phys Geogr* 37(6):476–510. <https://doi.org/10.1080/02723646.2016.1230986>
- Hai-Hoa N, McAlpine C, Pullar D, Johansen K, Duke NC (2013) The relationship of spatial–temporal changes in fringe mangrove extent and adjacent land-use: case study of Kien Giang coast, Vietnam, *Ocean Coast. Manage* 76:12–22
- Hapke CJ, Reid D, Richmond B (2009) Rates and trends of coastal change in California and the regional behavior of the beach and cliff system. *J Coast Res* 25:603–615
- Hasanuzzaman M, Gayen A, Shit PK (2022a) Channel dynamics and geomorphological adjustments of Kaljani River in Himalayan foothills. *Geocarto Int* 37(16):4687–4713. <https://doi.org/10.1080/10106049.2021.1882008>
- Hasanuzzaman M, Gayen A, Mafizul Haque S, Shit PK (2022b) Spatial modeling of river bank shifting and associated LULC changes of the Kaljani River in Himalayan foothills. *Stoch Environ Res Risk Assess.* <https://doi.org/10.1007/s00477-021-02147-1>
- Islam A, Guchhait SK (2017) Analysing the influence of Farakka Barrage Project on channel dynamics and meander geometry of Bhagirathi river of West Bengal, India. *Arab J Geosci* 10:245. <https://doi.org/10.1007/s12517-017-3004-2>
- Islam MR, Rahman MM, Akanda AS, Hasan MM (2020) Assessment of bank erosion hazard along the Brahmaputra River in Bangladesh using the Bank Erosion Hazard Index (BEHI). *Nat Hazards* 102(1):105–121
- Jana S (2019) An automated approach estimation and prediction of riverbank shifting for flood-prone middle-lower course of the Subarnarekha River, India. *Int J River Basin Manag.* <https://doi.org/10.1080/15715124.2019.1695259>
- Kankara RS, Selvan SC, Markose VJ, Rajan B, Arockiaraj S (2015) Estimation of long and short term shoreline changes along Andhra Pradesh coast using remote sensing and GIS techniques. *Procedia Eng* 116:855–862. <https://doi.org/10.1016/j.proeng.2015.08.374>
- Khan S, Sinha R, Whitehead P, Sarkar S, Jin L, Futter MN (2018) Flows and sediment dynamics in the Ganga River under present and future climate scenarios. *Hydrol Sci J* 63(5):763–782. <https://doi.org/10.1080/02626667.2018.1447113>
- Kuleli T, Guneroglu A, Kararli F, Dihkan M (2011) Automatic detection of shoreline change on coastal Ramsar wetlands of Turkey. *Ocean Eng* 38:1141–1149
- Li R, Liu J, Felus Y (2001) Spatial modelling and analysis for shoreline change and coastal erosion monitoring. *Mar Geodesy* 24:1–12. <https://doi.org/10.1080/01490410121502>
- Liu C, Wang D, Wu Y (2021) Vulnerability assessment of river embankments based on the REBVI method: a case study of the Gan River, China. *J Hydrol* 597:126157
- Majumdar S, Mandal S (2020) Assessment of relationship of braiding intensities with stream power and bank erosion rate through Plan Form Index (PFI) method: a study on selected reaches of the upstream of Ganga River near Malda district, West Bengal, India. *Sustain Water Resour Manag.* <https://doi.org/10.1007/s40899-020-00462-z>
- Mazzorana B, Comiti F, Fuchs S (2010) Comparison of stream bank erosion assessment methods: a case study from the Eastern Italian Alps. *Geomorphology* 114(4):435–447
- Mondal J, Mandal S (2018) Monitoring changing course of the river Ganga and land-use dynamicity in Manikchak Diara of Malda district, West Bengal, India, using geospatial tools. *Spat Inf Res* 26(6):691–704. <https://doi.org/10.1007/s41324-018-0210-2>

- Mondal M, Bhuni GS, Shit PK (2012) Vulnerability analysis of embankment breaching. *Int J Geol Earth Environ Sci* 2(3):89–102
- Muhammad A, Shakir AS (2018) Prediction of river bank erosion and protection works in a Reach of Chenab River, Pakistan. *Arab J Geosci*. <https://doi.org/10.1007/s12517-018-3493-7>
- Mukherjee K, Pal S (2017) Channel migration zone mapping of the River Ganga in the Diara surrounding region of Eastern India. *Environ Dev Sustain* 20(5):2181–2203. <https://doi.org/10.1007/s10668-017-9984-y>
- Mukhopadhyay A, Mukherjee S, Mukherjee S, Ghosh S, Hazra S, Mitra D (2012) Automatic shoreline detection and future prediction: a case study on Puri Coast, Bay of Bengal, India. *Eur J Remote Sens* 45(1):201–213. <https://doi.org/10.5721/eujrs20124519>
- Natesan U, Thulasiraman N, Deepthi K, Kathiravan K (2013) Shoreline change analysis of Vedaranyam coast, Tamil Nadu, India. *Environ Monit Assess* 185:5099–5109
- Pal R, Pani P (2019) Remote sensing and GIS-based analysis of evolving planform morphology of the middle-lower part of the Ganga River, India. *Egypt J Remote Sens Space Sci* 22(1):1–10. <https://doi.org/10.1016/j.ejrs.2018.01.007>
- Rahman AF, Dragoni D, El-Masri B (2011) Response of the Sundarbans coastline to sea level rise and decreased sediment flow: a remote sensing assessment. *Remote Sens Environ* 115:3121–3128
- Raj C, Singh V (2020) Assessment of planform changes of the Ganga River from Bhagalpur to Farakka during 1973–2019 using satellite imagery. *ISH J Hydraul Eng*. <https://doi.org/10.1080/09715010.2020.1812123>
- Rosgen DL (2001) A stream channel stability assessment methodology. In: 7th federal interagency sediment conference, March 25–29, Reno, Nevada
- Rosgen DL (2006) A watershed assessment for river stability and sediment supply (WARSSS). Wildland Hydrology Books. Fort Collins, Colorado
- Rudra K (2010) Dynamics of The Ganga in West Bengal, India (1764–2007): implications for science-policy interaction. *Quatern Int* 227(2):161–169. <https://doi.org/10.1016/j.quaint.2009.10.043>
- Sarif M, Siddiqui L, Islam M, Parveen N, Saha M (2021) Evolution of river course and morphometric features of the river Ganga: a case study of up and downstream of Farakka Barrage. *Int Soil Water Conserv Res* 9(4):578–590. <https://doi.org/10.1016/j.iswcr.2021.01.006>
- Simpson A, Turner I, Brantley E, Helms B (2014) Bank erosion hazard index as an indicator of near-bank aquatic habitat and community structure in a southeastern Piedmont stream. *Ecol Ind* 43:19–28. <https://doi.org/10.1016/j.ecolind.2014.02.002>
- Singh M, Singh IB, Müller G (2007) Sediment characteristics and transportation dynamics of the Ganga River. *Geomorphology* 86(1–2):144–175. <https://doi.org/10.1016/j.geomorph.2006.08.011>
- Sinha R, Ghosh S (2012) Understanding dynamics of large rivers aided by satellite remote sensing: a case study from lower Ganga Plains, India. *Geocarto Int* 27(3):207–219. <https://doi.org/10.1080/10106049.2011.620180>
- Talukdar S, Pal S, Singha P (2021) Proposing artificial intelligence based livelihood vulnerability index in river islands. *J Clean Prod* 284:124707
- Thakur P, Laha C, Aggarwal S (2011) River bank erosion hazard study of river Ganga, upstream of Farakka barrage using remote sensing and GIS. *Nat Hazards* 61(3):967–987. <https://doi.org/10.1007/s11069-011-9944-z>
- Thieler ER, Himmelstoss EA, Zichichi JL, Ergul A (2009) Digital Shoreline analysis system (DSAS) version 4.0—an ArcGIS extension for calculating shoreline change: U.S. Geological Survey Open-File Report 2008-1278
- Wang X, He S, Li Y, Zhang W (2020) An improved river embankment breaching vulnerability index (REBVI) model based on a grey system theory and entropy weight method. *J Hydrol* 590:125348. <https://doi.org/10.1016/j.jhydrol.2020.125348>
- Zheng Y, Tang L, Wang H (2021) An improved approach for monitoring urban built-up areas by combining NPP-VIIRS nighttime light, NDVI, NDWI, and NDBI. *J Clean Prod* 328:129488

**Publisher's Note** Springer Nature remains neutral with regard to jurisdictional claims in published maps and institutional affiliations.

Springer Nature or its licensor (e.g. a society or other partner) holds exclusive rights to this article under a publishing agreement with the author(s) or other rightsholder(s); author self-archiving of the accepted manuscript version of this article is solely governed by the terms of such publishing agreement and applicable law.

## Authors and Affiliations

Md Hasanuzzaman<sup>1</sup> · Biswajit Bera<sup>2</sup> · Aznarul Islam<sup>3</sup> · Pravat Kumar Shit<sup>1</sup> 

✉ Pravat Kumar Shit  
pravatgeo2007@gmail.com

Md Hasanuzzaman  
hasan20geo@gmail.com

Biswajit Bera  
biswajitbera007@gmail.com

Aznarul Islam  
aznarul\_geog@aliah.ac.in

<sup>1</sup> PG Department of Geography, Raja N. L. Khan Women's College (Autonomous), Gope Palace, Midnapore, West Bengal 721102, India

<sup>2</sup> Department of Geography, Sidho Kanho Birsha University, Puruliya, West Bengal, India

<sup>3</sup> Department of Geography, Aliah University, 17 Gorachand Road, Kolkata, West Bengal 700 014, India